Effect of Nitric Oxide in Amyloid Fibril Formation on Transthyretin-Related Amyloidosis†

Shiori Saito,‡ Yukio Ando,*,§ Masaaki Nakamura,§ Mitsuharu Ueda,|| Jaemi Kim,⊥ Yu Ishima,‡ Takaaki Akaike,@ and Masaki Otagiri‡

Department of Biopharmaceutics and Department of Molecular Medicine, Graduate School of Pharmaceutical Science, and Department of Diagnostic Medicine, Department of Neurology, and Department of Microbiology, Graduate School of Medical Sciences, Kumamoto University, Kumamoto, Japan

Received February 22, 2005; Revised Manuscript Received June 22, 2005

ABSTRACT: Although oxidative stress is said to play an important role in the amyloid formation mechanism in several types of amyloidosis, few details about this role have been described. Amyloid is commonly deposited around the vessels that are the primary site of action of nitric oxide generated from endothelial cells and smooth muscle cells, so nitric oxide may be also implicated in amyloid formation. For this study, we examined the in vitro effect of S-nitrosylation on amyloid formation induced by wild-type transthyretin, a precursor protein of senile systemic amyloidosis, and amyloidogenic transthyretin V30M, a precursor protein of amyloid deposition in familial amyloidotic polyneuropathy. S-Nitrosylation of amyloidogenic transthyretin V30M via the cysteine at position 10 was 2 times more extensive than that of wild-type transthyretin in a nitric oxide-generating solution. Both wild-type transthyretin and amyloidogenic transthyretin V30M formed amyloid fibrils under acidic conditions, and *S*-nitrosylated transthyretins exhibited higher amyloidogenicity than did unmodified transthyretins. Moreover, *S*-nitrosylated amyloidogenic transthyretin V30M formed more fibrils than did *S*-nitrosylated wild-type transthyretin. Structural studies revealed that S-nitrosylation of amyloidogenic transthyretin V30M induced a change in its conformation, as well as instability of the tetramer conformation. These results suggest that the nitric oxide-mediated modification of transthyretin, especially variant transthyretin, may play an important role in amyloid formation in senile systemic amyloidosis and familial amyloidotic polyneuropathy.

Progress in molecular genetics and biochemical methodologies has led to the identification of various types of amyloidosis and related amyloidogenic precursor proteins (*1*, *2*). However, the precise mechanism of amyloid formation remains to be elucidated. Familial amyloidotic polyneuropathy (FAP),[1] which is induced by amyloidogenic transthyretin (ATTR), is characterized by systemic accumulation of amyloid fibrils in the peripheral nerves and other organs (*3*, *4*). Of the different types of ATTR-related amyloidosis, FAP ATTR V30M is most common (*3*−*5*). Because most of the transthyretin (TTR) is produced by the liver, progression of the disease can be halted by liver transplantation (*6*−*9*). However, no other known therapy can prevent amyloid fibril formation in vivo, mainly because the mechanism of amyloid fibril formation in FAP is not well understood. In addition, amyloid deposits from elderly patients with systemic senile amyloidosis (SSA) have been proven to be derived from the wild-type (WT) TTR molecule. Details of the amyloid formation mechanism in SSA have also not been clarified (*10*).

Injury caused by free radicals has been implicated in the amyloid formation process in several types of systemic amyloidosis and localized amyloidosis, such as Alzheimer's disease (*11*, *12*), β_2-microglobulin amyloidosis (*13*), and FAP (*14*), and administration of scavengers of these free radicals has been suggested as a method of preventing amyloid fibril formation (*15*). Of the reactive oxygen species, reactive nitrogen species such as peroxynitrite and nitrogen dioxide have been proposed to be involved in the etiology of diverse pathophysiological conditions, including inflammation, neu-

† The authors' work was supported by grants from the Amyloidosis Research Committee, the Pathogenesis, Therapy of Hereditary Neuropathy Research Committee, the Surveys and Research on Specific Disease, the Ministry of Health and Welfare of Japan, the Charitable Trust Clinical Pathology Research Foundation of Japan, and a Research for the Future Program Grant, as well as Grants-in-Aid for Scientific Research (B) 15390275 and (B) 16406027 from the Ministry of Education, Science, Sports and Culture of Japan.

* To whom correspondence should be addressed: Department of Diagnostic Medicine, Graduate School of Medical Sciences, Kumamoto University, 1-1-1 Honjo, Kumamoto 860-0811, Japan. Telephone: +81-96-373-5686. Fax: +81-96-373-5686. E-mail: yukio@kaiju.medic.kumamoto-u.ac.jp.

‡ Department of Biopharmaceutics, Graduate School of Pharmaceutical Science.

§ Department of Diagnostic Medicine, Graduate School of Medical Sciences.

|| Department of Neurology, Graduate School of Medical Sciences.

⊥ Department of Molecular Medicine, Graduate School of Pharmaceutical Science.

@ Department of Microbiology, Graduate School of Medical Sciences.

[1] Abbreviations: FAP, familial amyloidotic polyneuropathy; ATTR, amyloidogenic transthyretin; TTR, transthyretin; SSA, systemic senile amyloidosis; WT, wild-type; IAN, isoamyl nitrate; DTT, 1,4-dithiothreitol; DTNB, 5,5′-dithiobis(2-nitrobenzoic acid); cTTRs, TTRs that underwent the same procedure as the *S*-nitrosylated TTRs but without IAN; NOC18, 1-hydroxy-2-oxo-3,3′-bis(2-aminoethyl)-1-triazene; GSNO, *S*-nitrosoglutathione.

10.1021/bi050327i CCC: $30.25
Published on Web 07/30/2005

rodegenerative diseases, cardiovascular disorders, cancer, and amyloidosis (*16*, *17*). *S*-Nitrosothiols are adducts of nitric oxide ($NO^{\bullet}$) and thiol-containing compounds that are found in many mammalian tissues and may affect various physiological functions, including signal transduction and immune responses (*18*). The bioactivities of low-molecular-weight *S*-nitrosothiols may be mediated either by their decomposition to $NO^{\bullet}$ or by direct exchange of their nitrosonium cation (NO^{+}) function with thiol-containing proteins (transnitrosylation) (*19*).

TTR forms tetramers with thyroxine and retinol-binding protein. Tetramers of amyloidogenic variants of TTR have been suggested to be more unstable than those of WT TTR (*20*), and partial acidic denaturation of the tetramers leads to formation of monomeric amyloidogenic intermediates (*21*). In addition, post-translational modification of TTR is also known to lead to amyloid fibril formation more easily than in native TTRs (*22*−*24*). TTR has one cysteine (Cys) at position 10, which is prone to undergoing several post-translational modifications such as cysteinylation, sulfonation, glutathionation, and nitrosylation. In addition, structural analysis has revealed that the Cys residue of ATTR V30M is located more to the outside of the molecule, which suggests that ATTR V30M may undergo modifications more frequently than the WT TTR via the Cys moiety (*25*). The variant TTR is a more highly amyloidogenic protein than WT TTR; the difference in the degree of post-translational modification between WT TTR and variant TTR also explained the amyloid fibril formation in FAP and SAA (*25*).

We recently reported the existence of oxidative stress in deposits of amyloid in tissues of patients with FAP as well as in those with other amyloidoses (*14*). Nitrotyrosine, a product of nitration, has also been reported to be present around amyloid deposited in transgenic mice with ATTR V30M (*26*). These results suggest that oxidative stress, especially that induced by NO, may play an important role in amyloid formation in FAP.

The aim of this study was to elucidate the effect of NO on amyloid fibril formation in FAP and SSA. We used biochemical methods to compare, in the presence or absence of S-nitrosylation, the degree of amyloid formation induced by both types of TTRs after changes in TTR structure, as well as the stability of the tetrameric forms of both TTRs.

EXPERIMENTAL PROCEDURES

Materials. Both WT TTR and ATTR V30M were purified from serum samples obtained from healthy volunteers and homozygotic FAP ATTR V30M patients as described previously (*27*). A brief description of this method follows.

Cold Ethanol Fractionation. Pooled serum samples from normal volunteers and homozygotic FAP ATTR V30M patients (200 mL) were mixed for 1 h at −5 °C with 8% ethanol at pH 7.5 and were then centrifuged at 10000*g* for 30 min. The supernatant was mixed for 1 h at −5 °C with 21% ethanol at pH 6.8 and was then centrifuged at 10000*g* for 30 min. This supernatant was dialyzed against 50 mM Tris-HCl (pH 7.6) and was then concentrated to 2 mL by ultrafiltration by using a Minisette Model ultrafiltration apparatus (Pall Technical Center, Port Washington, NY) and an OMEGA 10 kDa cutoff membrane (Filtron, Carbondale, PA). The resulting crude TTR preparation was used as the starting material in further purification steps. Affinity chromatography with 3 mg of human retinol-binding protein (Cortex Biochem, San Leandro, CA) was linked to 1.0 mL of HiTrap NHS-activated Sepharose 4FF (Amersham Pharmacia Biotech, Tokyo, Japan) according to Amersham Pharmacia Biotech's standard protocol. The column was equilibrated with 50 mM Tris-HCl (pH 7.6). A sample of 2 mL of starting material was applied to the column, and flow-through fractions with absorbance at 280 nm of more than 0.1 were collected as TTR-enriched fractions.

Anion-Exchange Column Chromatography. A 50 mL sample of the TTR-enriched fractions was passed through a 1.0 mL Resource Q column (Amersham Pharmacia Biotech) equilibrated with 50 mM Tris-HCl (pH 7.6). Unbound material was washed out with 50 mM Tris-HCl (pH 7.6) containing 70 mM NaCl. The bound fraction (crude TTR) was eluted with 50 mM Tris-HCl (pH 7.6) containing 200 mM NaCl, and was then concentrated to 5 mL by ultrafiltration with the Minisette Model ultrafiltration apparatus.

Removal of Albumin by Affinity Chromatography with Anti-Human Albumin Antibody. Anti-human albumin antibody (ICN, Tokyo, Japan) (25 mg) was linked to 5.0 mL of HiTrap NHS-activated Sepharose 4FF (Amersham Pharmacia Biotech) according to Amersham Pharmacia Biotech's standard protocol. The column was equilibrated with 50 mM Tris-HCl (pH 7.6) containing 0.3 M NaCl. An aliquot (5 mL) of the crude TTR-enriched fraction was passed through this column, and TTR devoid of albumin in the flow-through fractions was collected.

Gel Filtration Chromatography. The partially purified TTR from the anti-human albumin affinity chromatography column was concentrated to 2 mL by ultrafiltration on a Centriplus-10 concentrator (Millipore, Bedford, MA). This material was applied to a TSK gel G3000SW column (10 mm × 60 cm) (Tosoh, Tokyo, Japan) equilibrated with 50 mM sodium acetate buffer (pH 6.7) containing 0.3 M NaCl, at a flow rate of 5 mL/min. The TTR peak was collected at an elution time of approximately 30 min. This sample was then concentrated to 2 mL by ultrafiltration on a Centricon-10 concentrator (Millipore), after which the concentrated sample was dialyzed against 0.15 M NaCl.

Analysis of the Purity by Sodium Dodecyl Sulfate−*Polyacrylamide Gel Electrophoresis (SDS*−*PAGE) and High-Pressure Liquid Chromatography (HPLC).* SDS−PAGE (TEFCO, Tokyo, Japan) was performed as previously described by Harmansen et al. (*28*). Gels were stained with Coomassie Brilliant Blue R-250. HPLC analysis (*29*) was performed on a TSK gel G3000SWXL column (4.6 mm × 30 cm) (Tosoh) equilibrated with 20 mM sodium phosphate buffer (pH 7.0) containing 150 mM NaCl, at a flow rate of 0.4 mL/min.

S-Nitrosylation of WT TTR and ATTR V30M. WT TTR and ATTR V30M were *S*-nitrosylated by using isoamyl nitrate (IAN) from Wako (Osaka, Japan) as described previously (*30*−*32*). Before S-nitroylation of TTRs, each TTR (20 μM) was treated with 200 μM 1,4-dithiothreitol (DTT) in 100 mM sodium phosphate buffer (pH 7.4) with 5.0 mM ethylenediamine-*N*,*N*,*N*′,*N*′-tetraacetic acid at 37 °C for 5 min, followed by Sephadex G-25 column chromatography to obtain reduced forms of TTRs. The contents of the free cysteine of TTRs were ∼1 mol of the protein as determined by the 5,5′-dithiobis(2-nitrobenzoic acid) (DTNB)

method (*33*). DTT-treated TTRs (20 μM) were then reacted with 200 μM IAN in 100 mM sodium phosphate buffer (pH 7.8) containing 0.5 mM diethylenetriamine pentaacetic acid at 37 °C for 1 h. *S*-Nitrosylated products were purified by Sephadex G-25 gel filtration and eluted with 100 mM sodium phosphate buffer (pH 7.4). TTRs that underwent the same procedure as the *S*-nitrosylated TTRs but without IAN (cTTRs) were also made in an effort to compare their reactivities with those of *S*-nitrosylated TTRs.

Determination of S-Nitrosothiols Levels in WT TTR and ATTR V30M. *S*-Nitroso compounds formed in the reaction mixture were analyzed by means of the HPLC flow reactor system to identify *S*-nitrosothiols. *S*-Nitroso compounds, including *S*-nitroso proteins eluted from the HPLC column, were decomposed with Hg^{2+} and detected as nitrite (NO_2^-) after the reaction with the Griess reagent (*34*). A deproteinization column was used in this system for determination of *S*-nitroso protein levels just before the reaction with the Griess reagent. The stability of *S*-nitrosothiols associated with TTRs (Figure 3) was analyzed by a colorimetric assay using the Griess reagent according to Saville's method (*35*). Briefly, 50 μg of *S*-nitrosylated TTRs was incubated with a 10-fold molar excess of Hg^{2+} in 10 mM sodium acetate buffer (pH 5.5) at 37 °C for 30 min, and reacted with the Griess reagent at 40 °C for 10 min. The amount of NO_2^- released from each *S*-nitroso moiety was quantified with the Griess reagent reaction by measuring the absorbance at 540 nm. Simultaneously, 50 μg of the *S*-nitrosylated TTRs solution without Hg^{2+} treatment was reacted with the Griess reagent. The quantities of *S*-nitroso moieties in *S*-nitrosylated TTRs were assessed by comparing the absorbance observed with Hg^{2+}-untretaed *S*-nitrosylated TTRs to that of Hg^{2+}-tretaed *S*-nitrosylated TTRs.

Measurements of Circular Dichroism (CD) Spectra. CD spectra were obtained by using a JASCO (Tokyo, Japan) J-720 spectropolarimeter at 25 °C. A molecular mass of TTR of 14 kDa was used for calculation of the mean residue ellipticity. Far-UV and CD spectra were recorded at a protein concentration of 10 μM, in 67 mM sodium phosphate (pH 7.4).

Tryptophan (Trp) Fluorescence Intensity. The fluorescence intensity of Trp was measured via a Hitachi (Tokyo, Japan) F-4500 spectrofluorimeter at 25 °C. All assays used excitation at 295 nm and emission at 340 nm. Excitation and emission slits were set at 5 nm. The fluorescence intensity was recorded at a protein concentration of 10 μM, in 67 mM sodium phosphate (pH 7.4).

Amyloid Formation Induced by WT TTR and ATTR V30M. To evaluate amyloid fibril formation after S-nitrosylation, unmodified or *S*-nitrosylated WT TTR and ATTR V30M were diluted in 50 mM sodium acetate and 100 mM NaCl at the desired pH (3.0−6.5) in an Eppendorf tube to obtain a final TTR concentration of 15 μM. The resulting stationary solutions were incubated at 37 °C for 5 days in the dark (*36*).

Thioflavin T-Based Fluorimetric Assays. To assess the amount of amyloid fibrils in vitro, the thioflavin T test has been widely used (*37*, *38*). Fluorescence spectra were obtained by using a Hitachi F-4500 spectrofluorimeter with an assay volume of 1 mL. All assays used excitation at 450 nm and emission at 482 nm. Excitation and emission slits were set at 5 nm. The reaction mixture contained 5 μM thioflavin T and 50 mM Gly-NaOH buffer (pH 10.0) (*37*, *38*). Ten microliters of a 15 μM WT TTR or ATTR V30M solution was added to 1 mL of the reaction mixture. Spectra were recorded at 25 °C within minutes of the addition of the sample to the reaction mixture.

Amyloid Formation from TTRs in the Presence of Exogenous NO. To examine the direct effect of NO on the amyloidogenicity of TTRs, TTRs were reacted with various NO (NO^+)-releasing reagents, such as 1-hydroxy-2-oxo-3,3-bis(2-aminoethyl)-1-triazene (NOC18; Dojindo Laboratories, Kumamoto, Japan) and *S*-nitrosoglutathione (GSNO) (*39*). Samples of 15 μM unmodified or *S*-nitrosylated WT TTR and ATTR V30M were incubated in 50 mM sodium acetate and 100 mM NaCl at pH 3.0 in the presence or absence of 50 μM NOC18 and GSNO at 37 °C in the dark for 5 days. Amyloidogenicity was examined under the same conditions that are described above.

Nonboiled (Nonreducing) SDS−PAGE. Nonboiled SDS−PAGE was performed under nondenaturing conditions. One microgram of the TTR samples incubated for 37 °C for 5 days at pH 3.0 as described above was neutralized with PBS to obtain a final pH of >6.5. After neutralization, samples were mixed with 5% SDS sample buffer and loaded on 15% polyacrylamide gels, which were stained with Coomassie Brilliant Blue. Band intensities were evaluated by densitometric analysis using ATTO densito (ATTO, Tokyo, Japan).

Statistical Analysis. Statistical evaluation was performed by means of the paired *t* test. A p value of <0.05 was taken to be statistically significant.

RESULTS

Ratio of S-Nitrosylation of TTR Molecules. The ratio of S-nitrosylation of TTRs was determined by titrating *S*-nitrosothiol levels. The ratio of *S*-nitrosothiols for ATTR V30M was much higher than that for WT TTR (WT TTR, 0.39 mol/mol of protein; ATTR V30M, 0.67 mol/mol of protein). Dissociation of tetrameric forms to monomeric forms in TTRs was not recognized by nonreducing SDS−PAGE (data not shown).

Conformational Changes of S-Nitrosylated TTRs. The conformations of *S*-nitrosylated WT TTR and ATTR V30M were compared with those of unmodified TTRs by means of CD. Unmodified and *S*-nitrosylated WT TTR and ATTR V30M showed no significant difference in conformation in far-UV spectral analyses (Figure 1). However, S-nitrosylation of WT TTR induced a slight change in Trp fluorescence intensity at the 340 nm wavelength. Moreover, the Trp fluorescence intensity for *S*-nitrosylated ATTR V30M decreased to a greater degree compared with the change in Trp fluorescence intensity for WT TTR (Figure 2). CD spectra and the Trp fluorescence intensity of cTTRs did not significantly differ from that of unmodified TTRs (data not shown).

Stability of S-Nitrosothiol Associated with TTRs. The stability of *S*-nitrosothiol associated with WT TTR and ATTR V30M was measured at pH 3.0 (Figure 3A) and pH 7.0 (Figure 3B) in the dark. NO associated with TTR dissociated from the protein in a time-dependent manner: dissociation from TTR molecules started just after incubation began, and little NO remained associated with both TTRs after day 10 at pH 3.0 (Figure 3A). At pH 3.0, the half-life

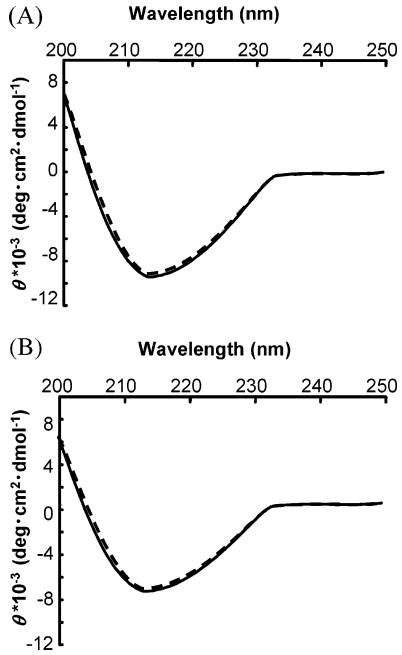

FIGURE 1: Far-UV CD spectral analysis. Samples (1.5 mL) of unmodified or *S*-nitrosylated WT TTR and ATTR V30M [10 μM in 67 mM sodium phosphate (pH 7.4)] were applied to a JASCO J-720 spectropolarimeter as described in the text. (A) Unmodified WT TTR (—) and its *S*-nitrosylated form (– – –). (B) Unmodified ATTR V30M (—) and its *S*-nitrosylated form (– – –).

of *S*-nitrosylated TTRs was 6.6 days in WT TTR and 6.3 days in ATTR V30M. In contrast, at pH 7.0, more than 60% of NO associated with WT TTR and ATTR V30M remained unchanged 15 days after incubation started (Figure 3B). At pH 7.0, the half-life of *S*-nitrosylated TTRs was 22.05 days in WT TTR and 18.3 days in ATTR V30M. At both pH, *S*-nitrosothiols were more rapidly decayed in ATTR V30M than in WT TTR.

Effect of S-Nitrosylation on Amyloid Formation Induced by TTRs. The effect of S-nitrosylation on amyloid formation induced by WT TTR and ATTR V30M was evaluated by means of the thioflavin T-based test as described above. Both WT TTR and ATTR V30M exhibited increased fluorescence intensity as the pH of the incubation solution decreased (Figure 4). The fluorescence intensity of unmodified ATTR V30M was higher than that of WT TTR, and both *S*-nitrosylated TTRs had a higher intensity than unmodified TTRs. In addition, *S*-nitrosylated ATTR V30M exhibited greater fluorescence intensity than *S*-nitrosylated WT TTR. The fluorescence intensity of cTTRs did not significantly differ from that of unmodified TTRs (data not shown).

Amyloid Formation of TTRs in the Presence of Exogenous NO. To determine whether formation of *S*-nitrothiols or direct inhalation of the proteins with NO affected amyloid fibril formation during incubation of *S*-nitrosylated TTRs, unmodified TTR and ATTR V30M were incubated with NOC18 or GSNO at pH 3.0 and 37 °C in the dark for 5 days, and amyloidogenicity was compared by means of the thioflavin T-based test. As demonstrated in Figure 5, TTRs incubated with NOC18 under acidic conditions showed no significant increase in the extent of amyloid formation, compared with unmodified TTRs. *S*-Nitrosylated WT TTR and *S*-nitrosylated ATTR V30M and ATTR V30M incubated with GSNO exhibited greater amyloidogenicity than unmodified TTR and

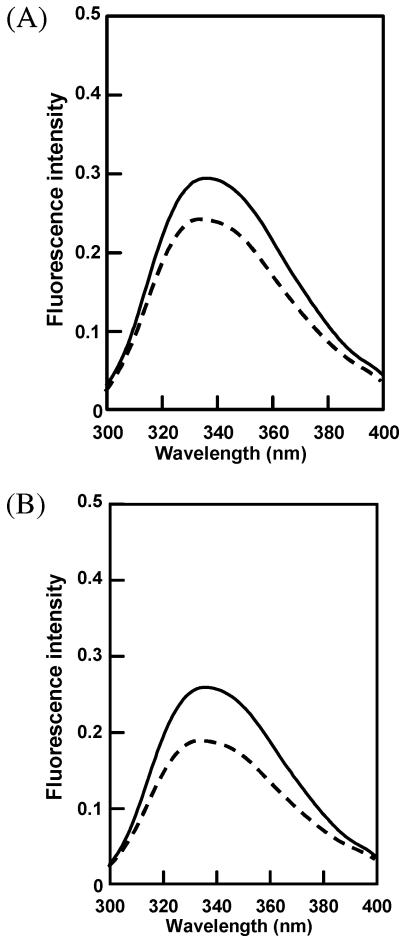

FIGURE 2: Trp fluorescence intensity of TTRs. The Trp fluorescence intensities of unmodified or *S*-nitrosylated WT TTR and ATTR V30M were monitored by using a Hitachi F-4500 spectropolarimeter. Aliquots of 2 mL of 10 μM WT TTR and ATTR V30M [in 67 mM sodium phosphate (pH 7.4)] were used in the experiments. (A) Unmodified WT TTR (—) and its *S*-nitrosylated form (– – –). (B) Unmodified ATTR V30M (—) and its *S*-nitrosylated form (– – –).

NOC18-treated TTR (unmodified ATTR V30M vs *S*-nitrosylated ATTR V30M, $p < 0.01$).

Effect of S-Nitrosylation on the Stability of the Tetrameric Form of TTRs. To examine the effect of S-nitrosylation on the stability of the tetrameric form of TTRs, nonboiled (nonreducing) SDS−PAGE was performed with unmodified and *S*-nitrosylated TTRs (Figure 6A). The ratio of the monomeric band to the tetrameric band was decreased in *S*-nitrosylated TTR, especially ATTR V30M. Figure 6B presents quantified results and shows that *S*-nitrosylated TTRs had greater proportions of monomers than did unmodified TTRs. The *S*-nitrosylated ATTR V30M exhibited the highest ratio of monomer to tetramer.

DISCUSSION

We demonstrated here that *S*-nitrosylated TTRs possessed increased amyloidogenicity in the amyloid-generating system in vitro, compared with unmodified TTRs, and that *S*-nitrosylated ATTR V30M induced more amyloid fibrils than did WT TTR. Conformational analyses have documented that Cys at position 10 in ATTR V30M is situated more to the outside of the molecule than in WT TTR (*25*). This finding suggested that the Cys of ATTR V30M may be more

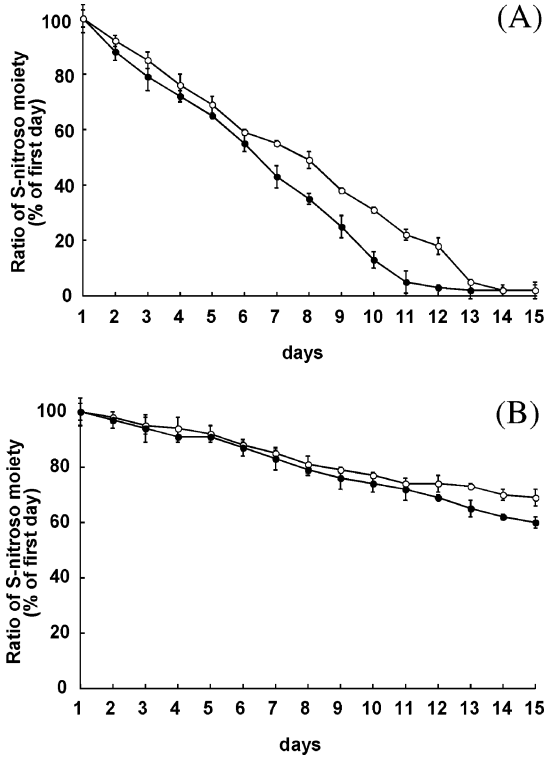

FIGURE 3: Stability of *S*-nitrosothiols associated with TTRs. This stability was examined until day 15 after the incubation started. *S*-Nitroso compounds formed in the reaction mixture were analyzed with the HPLC flow reactor system to identify *S*-nitrosothiols as described in the text. Samples of 50 μg of unmodified or *S*-nitrosylated WT TTR and ATTR V30M were used in the incubations at pH 3.0 (A) and pH 7.0 (B) and 37 °C in the dark: (○) WT TTR and (●) ATTR V30M.

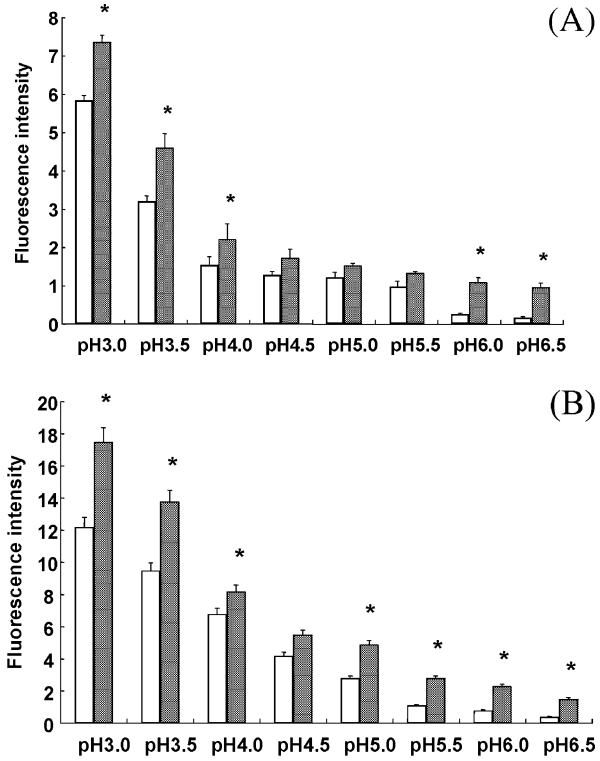

FIGURE 4: Effect of S-nitrosylation on amyloid formation induced by TTRs. Unmodified and *S*-nitrosylated WT TTR and ATTR V30M were diluted in 20 mM sodium acetate (pH 3.0−6.5) and 100 mM NaCl at the desired pH in an Eppendorf tube to obtain a final TTR concentration of 15 μM. The resulting stationary solutions were incubated at 37 °C for 5 days. The data were expressed as the increased values compared to those of the time just starting the incubation with (A) WT TTR and (B) ATTR V30M: (white columns) unmodified TTRs and (gray columns) *S*-nitrosylated TTRs. In panel A, an asterisk indicates that $p < 0.01$, for unmodified WT TTR vs *S*-nitrosylated WT TTR. In panel B, an asterisk indicates that $p < 0.01$, for unmodified ATTR V30M vs *S*-nitrosylated ATTR V30M.

accessible to NO and thus susceptible to S-nitrosylation. In fact, the extent of S-nitrosylation of ATTR V30M was greater than that of WT TTR. Figure 4 indicates that *S*-nitrosylated ATTR V30M exhibited a greater thioflavin T fluorescence intensity than did WT TTR after incubation under acidic conditions. These findings demonstrate that the amount of amyloid fibrils formed increased as the ratio of S-nitrosylation increased.

Conformational study of *S*-nitrosylated TTRs revealed that, although far-UV spectral analyses indicated no significant difference between unmodified and *S*-nitrosylated proteins (Figure 1), the Trp fluorescence intensity at the 340 nm wavelength was significantly decreased in *S*-nitrosylated TTRs compared with unmodified TTRs, and *S*-nitrosylated ATTR V30M showed a greater reduction in intensity compared with wild-type TTR (Figure 2). These results suggest that, although S-nitrosylation of Cys at position 10 may not have a great influence on TTR structure, this modification may affect the microstructure around Trp at positions 41 and 79.

We also examined the possibility of dissociation of NO from TTRs during incubation at different pHs (Figure 3). Although *S*-nitrosothiols formed in proteins and peptides appear to be stable under acidic conditions (*40*), *S*-nitrosylated TTRs were found to be labile in an acidic solution (pH 3.0). Specifically, more than 60% of *S*-nitrosylated WT TTR and ATTR V30M remained unchanged at pH 7.0 15 days after incubation began. However, at pH 3.0, NO started to dissociate from the TTR molecule, and little NO remained associated with the TTRs on day 15 at this pH value. At both pHs, *S*-nitrosothiols were more rapidly decayed in ATTR than in WT TTR. This NO dissociation may be induced by conformational changes of TTRs occurring at low pH, which facilitates dissociation of TTR tetramers to monomers. As demonstrated in Figure 6, in *S*-nitrosylated ATTR V30M, the ratio of monomeric forms to tetramers was much greater than in *S*-nitrosylated WT TTR.

In amyloid deposits in FAP as well as other amyloidoses, accumulation of human neutrophil elastase and cathepsin G derived from polymorphonuclear leukocytes has been documented (*41*). This result suggests that free radical species, including NO, may play a role in the amyloid formation mechanism in FAP. Therefore, it is quite important to elucidate whether the increased amyloidogenicity depends solely on the effect of S-nitrosylation of TTRs. We incubated both unmodified WT TTR and ATTR V30M with NOC18 or GSNO to generate NO or nitrosonium cation (NO^+) (*39*). The thioflavin T fluorescence intensity of TTRs did not significantly increase with NOC18 treatment. Incubation with GSNO, however, produced a significant increase in the thioflavin T fluorescence intensity of *S*-nitrosylated TTRs compared with unmodified and NOC18-incubated TTRs. Although NO generated from NOC18 cannot react with TTRs under acidic conditions, NO^+ generated from GSNO

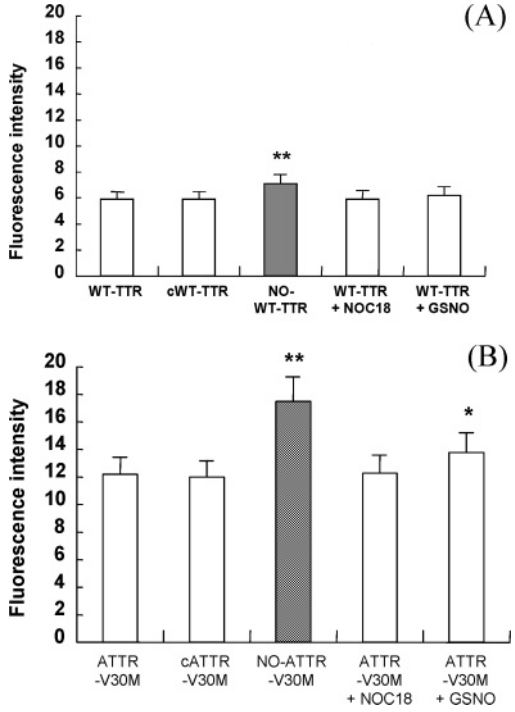

FIGURE 5: Amyloid formation of TTRs in the presence of exogenous NO. Samples of 15 μM unmodified or *S*-nitrosylated WT TTR and ATTR V30M were incubated in 50 mM sodium acetate and 100 mM KCl at pH 3.0 in the presence or absence of 50 μM NOC18 and GSNO. Amyloidogenicity was examined under the same conditions that are described in the legend of Figure 4: (A) WT TTR and (B) ATTR V30M. cTTRs are TTRs that underwent the same procedure as the *S*-nitrosylated TTRs but without IAN. Two asterisks indicate that $p < 0.01$, for unmodified TTRs vs *S*-nitrosylated TTRs at pH 3.0. One asterisk indicates that $p < 0.05$, for unmodified ATTR V30M vs TTR incubated with GSNO.

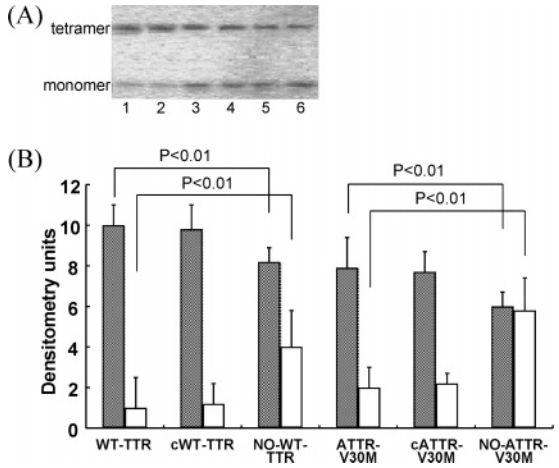

FIGURE 6: Effect of S-nitrosylation on the stability of the tetrameric forms of TTRs. Samples of 15 μM unmodified or *S*-nitrosylated WT TTR and ATTR V30M were incubated at 37 °C for 5 days in acetate buffer (pH 3.0). (A) Samples were analyzed via nonboiled (nonreducing) SDS−PAGE as described in the text: lane 1, WT TTR; lane 2, WT cTTR; lane 3, NO-bound WT TTR; lane 4, ATTR V30M; lane 5, cATTR V30M; and lane 6, NO-bound ATTR V30M. (B) Intensities of the bands were evaluated by densitometric analysis (ATTO densito, ATTO, Tokyo, Japan): (white columns) TTR monomers and (gray columns) TTR tetramers.

induces transnitrosylation, which occurs even at acidic pH, and in those solutions, TTRs may undergo S-nitrosylation (*19*). These results suggest that NO dissociated from TTR may not directly participate in amyloid fibril formation.

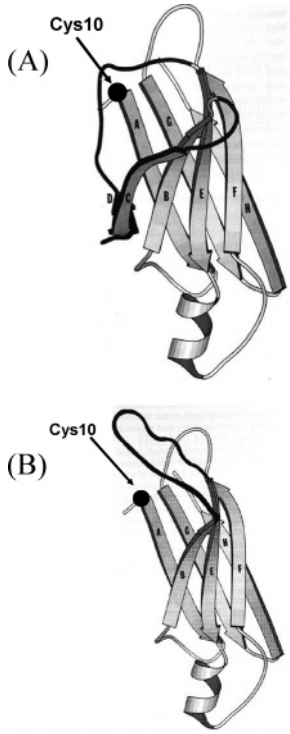

FIGURE 7: Conformation of WT TTR and ATTR V30M. A change in TTR structure caused by an amino acid substitution may induce amyloid formation by facilitating dissociation of TTR tetramers to monomers, which leads to amyloid fibril formation via misfolding C−D strands of the TTR molecule. S-Nitrosylation in TTRs may be one of the factors facilitating dissociation of TTR tetramers to monomers.

It is widely accepted that a change in TTR structure caused by an amino acid mutation may induce amyloid formation by facilitating dissociation of TTR tetramers to monomers (*42*) (Figure 7). To elucidate the mechanism of the increased amyloidogenicity in *S*-nitrosylated TTRs, we used nonboiled (nonreducing) SDS−PAGE to examine the ratio of tetramers to monomers for *S*-nitrosylated WT TTR and ATTR V30M. As Figure 6 shows, *S*-nitrosylated TTRs had higher ratios of monomeric to tetrameric forms than did unmodified TTRs, and the proportion of the monomeric form of *S*-nitrosylated ATTR V30M was greater than that of *S*-nitrosylated WT TTR. These results indicate that the increase in the extent of monomer formation occurs depending on S-nitrosylation of TTRs. This analysis and other conformational studies thus suggest that S-nitrosylation of TTRs induced a change in TTR structure, leading to reduced tetrameric stability and enhancing the amyloidogenicity of TTRs.

Unmodified Cys residues of circulating plasma proteins such as albumin and α_1-protease inhibitor undergo S-nitrosylation, and these *S*-nitrosylated proteins protect against tissue injury (*43*). However, as Figure 5 demonstrates, *S*-nitrosylated TTR would function as a harmful protein for amyloid fibril formation, whereas *S*-nitrosylated TTR in the bloodstream may work as a beneficial molecule for tissue injury, like *S*-nitrosylated albumin and α_1-protease inhibitor (*18*, *44*, *45*). Further study is needed.

In all types of TTR-related FAP, perivascular sites are known to show the greatest level of amyloid deposition, although the reason for this finding has not been well explained. These lesions are locations of NO reactions, where endothelial cells of vessels and smooth muscles generate NO.

In fact, nitrotyrosine antibody exhibited perivascular immunoreactivity at sites of abundant amyloid deposition in transgenic mice with ATTR V30M (*26*).

In conclusion, ATTR V30M was more prone to undergoing S-nitrosylation than WT TTR. *S*-Nitrosylated TTRs, especially ATTR V30M, induced formation of amyloid fibrils after a change in conformation. FAP, whose precursor protein is primarily ATTR V30M, usually starts to produce clinical manifestations when patients are ~35−45 years old; SSA, whose precursor protein is WT TTR, usually starts to produce clinical cardiac symptoms when patients are more than 80 years old (*10*). ATTR V30M is more prone than WT TTR to undergoing post-translational modification via the Cys residue at position 10. This distinction may contribute to the difference in the time of onset of these two types of systemic amyloidoses.

REFERENCES

1. Pepys, M. B., Hawkins, P. N., Booth, D. R., Vigushin, D. M., Tennent, G. A., Soutar, A. K., Totty, N., Nguyen, O., Blake, C. C., Terry, C. J., Feest, T. G., Zalin, A. M., and Hsuan, J. J. (1993) Human lysozyme gene mutations cause hereditary systemic amyloidosis, *Nature 362*, 553−557.
2. Westermark, P., Bergstrom, J., Solomon, A., Murphy, C., and Sletten, K. (2003) Transthyretin-derived senile systemic amyloidosis: Clinicopathologic and structural considerations, *Amyloid 10*, 48−54.
3. Benson, M. D., and Uemichi, T. (1996) Transthyretin amyloidosis, *Amyloid 3*, 44−56.
4. Ando, Y., Araki, S., and Ando, M. (1993) Transthyretin and familial amyloidotic polyneuropathy, *Intern. Med. (Tokyo, Jpn.) 32*, 920−922.
5. Ando, Y., Nakamura, M., and Araki, S. (2005) Transthyretin related familial amyloidotic polyneuropathy, *Arch. Neurol. 62*, 1−6.
6. Holmgren, G., Steen, L., Suhr, O., Ericzon, B. G., Groth, C. G., Anderson, O., Wallin, B. G., Seymour, A., Richardson, S., Hawkins, P. N., and Pepys, M. B. (1993) Clinical improvement and amyloid regression after liver transplantation in hereditary transthyretin amyloidosis, *Lancet 341*, 1113−1116.
7. Ando, Y., Tanaka, Y., Nakazato, M., Ericzon, B. G., Yamashita, T., Tashima, K., Sakashita, N., Suga, M., Uchino, M., and Ando, M. (1995) Change in variant transthyretin levels in patients with familial amyloidotic polyneuropathy type I following liver transplantation, *Biochem. Biophys. Res. Commun. 211*, 354−358.
8. Ando, Y., Tanaka, Y., Ando, E., Yamashita, T., Nishida, Y., Tashima, Y., Suga, M., Uchino, M., and Ando, M. (1995) Effect of liver transplantation on autonomic dysfunction in familial amyloidotic polyneuropathy type I, *Lancet 345*, 195−196.
9. Skinner, M., Lewis, W. D., Jones, L. A., Kasirsky, J., Kane, K., Ju, S. T., Jenkins, R., Falk, R. H., Simms, R. W., and Cohen, A. S. (1994) Liver transplantation as a treatment for familial amyloidotic polyneuropathy, *Ann. Intern. Med. 120*, 133−134.
10. Cornwell, G. G., III, Sletten, K., Johansson, B., and Westermark, P. (1988) Evidence that the amyloid fibril protein in senile systemic amyloidosis is derived from normal prealbumin, *Biochem. Biophys. Res. Commun. 154*, 648−653.
11. Schoneich, C. (2002) Redox processes of methionine relevant to β-amyloid oxidation and Alzheimer's disease, *Arch. Biochem. Biophys. 397*, 370−376.
12. Rosenblum, W. I. (2002) Structure and location of amyloid β peptide chains and arrays in Alzheimer's disease: New findings require reevaluation of the amyloid hypothesis and of tests of the hypothesis, *Neurobiol. Aging 23*, 225−230.
13. Descamps-Latscha, B., Jungers, P., and Witko-Sarsat, V. (2002) Immune system dysregulation in uremia: Role of oxidative stress, *Blood Purif. 20*, 481−484.
14. Ando, Y., Nyhlin, N., Suhr, O., Holmgren, G., Uchida, K., El-Sahly, M., Yamashita, T., Terasaki, H., Nakamura, M., Uchino, M., and Ando, M. (1997) Oxidative stress is found in amyloid deposits in systemic amyloidosis, *Biochem. Biophys. Res. Commun. 232*, 497−502.
15. Suhr, O., Lang, K., Wikstrom, L., Anan, I., Ando, Y., El-Salhy, M., Holmgren, G., and Tashima, K. (2001) Scavenger treatment of free radical injury in familial amyloidotic polyneuropathy: A study on Swedish transplanted and non-transplanted patients, *Scand. J. Clin. Lab. Invest. 61*, 11−18.
16. Ferdinandy, P. (2004) Nitric oxide and peroxynitrite in cardioprotection: The effect of hyperlipidaemia, *Cardiovasc. J. S. Afr. 15*, S4.
17. Berg, D., Youdim, M. B., and Riederer, P. (2004) Redox imbalance, *Cell Tissue Res. 318*, 201−213.
18. Akaike, T., and Maeda, H. (2000) Nitric oxide and virus infection, *Immunology 101*, 300−308.
19. Kikugawa, K., Hiramoto, K., and Ohkawa, T. (2004) Effects of oxygen on the reactivity of nitrogen oxide species including peroxynitrite, *Biol. Pharm. Bull. 27*, 17−23.
20. McCutchen, S. L., Lai, Z., Miroy, G. J., Kelly, J. W., and Colon, W. (1995) Comparison of lethal and nonlethal transthyretin variants and their relationship to amyloid disease, *Biochemistry 34*, 13527−13536.
21. Kelly, J. W., Colon, W., Lai, Z., Lashuel, H. A., McCulloch, J., McCulloch, S. L., Miroy, G. J., and Peterson, P. A. (1997) Transthyretin quaternary and tertiary structural changes facilitate misassembly into amyloid, *Adv. Protein Chem. 50*, 161−181.
22. Ando, Y., Ohlsson, P. I., Suhr, O., Nyhlin, N., Yamashita, T., Holmgren, G., Danielsson, A., Sansgren, O., Uchino, M., and Ando, M. (1996) A new simple and rapid screening method for variant transthyretin-related amyloidosis, *Biochem. Biophys. Res. Commun. 228*, 480−483.
23. Kishikawa, M., Nakanishi, T., Miyazaki, A., Shimizu, A., Kusaka, H., Fukui, M., and Nishiue, T. (1999) A new amyloidogenic transthyretin variant, [D38A], detected by electrospray ionization/mass spectrometry, *Amyloid 6*, 183−186.
24. Takaoka, Y., Ohta, M., Miyakawa, K., Nakamura, O., Suzuki, M., Takahashi, K., Yamamura, K., and Sakaki, Y. (2004) Cysteine 10 is a key residue in amyloidogenesis of human transthyretin Val30Met, *Am. J. Pathol. 164*, 337−345.
25. Zhang, Q., and Kelly, J. W. (2003) Cys10 mixed disulfides make transthyretin more amyloidogenic under mildly acidic conditions, *Biochemistry 42*, 8756−8761.
26. Sousa, M. M., Fernandes, R., Palha, J. A., Taboada, A., Vieira, P., and Saraiva, M. J. (2002) Evidence for early cytotoxic aggregates in transgenic mice for human transthyretin Leu55Pro, *Am. J. Pathol. 161*, 1935−1948.
27. Ando, Y., Yamashita, T., Nakamura, M., Tanaka, Y., Hashimoto, M., Tashima, K., Suhr, O., Uemura, Y., Obayashi, K., Terazaki, H., Suga, M., Uchino, M., and Ando, M. (1997) Down regulation of a harmful variant protein by replacement of its normal protein, *Biochim. Biophys. Acta 1362*, 39−46.
28. Hermansen, L. F., Bergman, T., Jornvall, H., Husby, G., Ranlov, I., and Sletten, K. (1995) Purification and characterization of amyloid-related transthyretin associated with familial amyloidotic cardiomyopathy, *Eur. J. Biochem. 227*, 772−779.
29. Quintas, A., Saraiva, M. J., and Brito, R. M. (1997) The amyloidogenic potential of transthyretin variants correlates with their tendency to aggregate in solution, *FEBS Lett. 418*, 297−300.
30. Miyamoto, Y., Akaike, T., and Maeda, H. (2000) S-Nitrosylated human α_1-protease inhibitor, *Biochim. Biophys. Acta 1477*, 90−97.
31. Akaike, T. (2000) Mechanisms of biological S-nitrosation and its measurement, *Free Radical Res. 33*, 461−469.
32. Inoue, K., Akaike, T., Miyamoto, Y., Okamoto, T., Sawa, T., Otagiri, M., Suzuki, S., Yoshimura, T., and Maeda, H. (1999) Nitrosothiol formation catalyzed by ceruloplasmin. Implication for cytoprotective mechanism in vivo, *J. Biol. Chem. 274*, 27069−27075.
33. Takabayashi, K., Imada, T., Saito, Y., and Inada, Y. (1983) Coupling between fatty acid binding and sulfhydryl oxidation in bovine serum albumin, *Eur. J. Biochem. 136*, 291−295.
34. Akaike, T., Inoue, K., Okamoto, T., Nishino, H., Otagiri, M., Fujii, S., and Maeda, H. (1997) Nanomolar quantification and identification of various nitrosothiols by high performance liquid chromatography coupled with flow reactors of metals and Griess reagent, *J. Biochem. 122*, 459−466.
35. Saville, B. (1958) A scheme for the colorimetric determination of microgram amounts of thiols, *Analyst 83*, 670−672.

36. Goldberg, M. E., Rudolph, R., and Jaenicke, R. (1991) A kinetic study of the competition between renaturation and aggregation during the refolding of denatured-reduced egg white lysozyme, *Biochemistry 30*, 2790−2797.
37. Bonifacio, M. J., Sasaki, Y., and Saraiva, M. J. (1996) 'In vitro' amyloid fibril formation from transthyretin: The influence of ions and the amyloidogenicity of TTR variants, *Biochim. Biophys. Acta 1316*, 35−42.
38. Naiki, H., Higuchi, K., Hosokawa, M., and Takeda, T. (1989) Fluorometric determination of amyloid fibrils in vitro using the fluorescent dye, thioflavin T1, *Anal. Biochem. 177*, 244−249.
39. del Rio, L. A., Corpas, F. J., Sandalio, L. M., Palma, J. M., Gomez, M., and Barroso, J. B. (2002) Reactive oxygen species, antioxidant systems and nitric oxide in peroxisomes, *J. Exp. Bot. 53*, 1255−1272.
40. Mirza, U. A., Chait, B. T., and Lander, H. M. (1995) Monitoring reactions of nitric oxide with peptides and proteins by electrospray ionization-mass spectrometry, *J. Biol. Chem. 270*, 17185−17188.
41. Skinner, M., Stone, P., Shirahama, T., Connors, L. H., Calore, J., and Cohen, A. S. (1986) The association of an elastase with amyloid fibrils, *Proc. Soc. Exp. Biol. Med. 181*, 211−214.
42. Jiang, X., Buxbaum, J. N., and Kelly, J. W. (2001) The V122I cardiomyopathy variant of transthyretin increases the velocity of rate-limiting tetramer dissociation, resulting in accelerated amyloidosis, *Proc. Natl. Acad. Sci. U.S.A. 98*, 14943−14948.
43. Jaffrey, S. R., Erdjument-Bromage, H., Ferris, C. D., Tempst, P., and Snyder, S. H. (2001) Protein S-nitrosylation: A physiological signal for neuronal nitric oxide, *Nat. Cell Biol. 3*, 193−197.
44. Foster, M. W., McMahon, T. J., and Stamler, J. S. (2003) S-nitrosylation in health and disease, *Trends Mol. Med. 9*, 160−168.
45. Jia, L., Bonaventura, C., Bonaventura, J., and Stanler, J. S. (1996) S-nitrosohaemoglobin: A dynamic activity of blood involved in vascular control, *Nature 380*, 221−226.

BI050327I